Urban Climate 24 (2018) 326–339

Contents lists available at ScienceDirect

Urban Climate

journal homepage: http://www.elsevier.com/locate/uclim

Using reflective pavements to mitigate urban heat island in warm climates - Results from a large scale urban mitigation project

G-E. Kyriakodis[a,*], M. Santamouris[a,b]

[a] Group Building Environmental Studies, Physics Department, University of Athens, Athens, Greece
[b] The Anita Lawrence Chair in High Performance Architecture, School of Built Environment, University of New South Wales, Sydney, Australia

ARTICLE INFO

Article history:
Received 14 October 2016
Received in revised form 3 February 2017
Accepted 7 February 2017
Available online 10 February 2017

Keywords:
Heat island
Cool materials and pavements
Cool coloured thin layer asphalt
Photocatalytic pavements
Heat island mitigation techniques
Urban climatic change

ABSTRACT

UHI is the most studied phenomenon of climate change and refers to the increased ambient temperature of cities compared to rural settings. Implementation of reflective materials to urban structures, such as roads and pavements, reduces the surface and ambient temperature and contributes to counterbalance the impact of the phenomenon. The present paper describes the design and the experimental evaluation of a large scale implementation of cool asphaltic and concrete pavements in a major traffic axis of Western Athens covering a total zone of 37,000 m^2. To our knowledge, this project is one of the largest urban mitigation projects in the world. Extended monitoring was performed in the area during the entirety of the summer period, while Computational Fluid Dynamics (CFD) simulation was used to evaluate the thermal impact of the application. It was concluded that the use of cool non-aged asphalt can reduce the ambient temperature by up to 1.5 °C and the maximum surface temperature reduction could reach 11.5 °C, while the thermal comfort conditions can improve considerably. Ageing phenomena may reduce substantially and up to 50% the mitigation potential of cool asphaltic materials.

1. Introduction

The urban heat island phenomenon refers to the increase of the ambient temperature of cities compared to their surrounding suburban and rural environment. Increased urban temperature is the result of the positive thermal balance of cities caused by the additional heat released and stored in the urban structure, and the lack of low temperature environmental sinks (Santamouris, 2001). The urban heat island is the most studied phenomenon of climate change, and there are more than 400 cities around the world where experimental documentation is available (Santamouris, 2015a, 2016b). The amplitude of the phenomenon varies as a function of the local characteristics and of the strength of the heat sources and may exceed 6–7 K (Santamouris and Kolokotsa, 2016).

Local climate change has a significant impact on the energy consumption of buildings, it increases the concentration of local pollutants, deteriorates indoor and outdoor thermal comfort conditions, increases the vulnerability of low-income

* Corresponding author.
E-mail address: gkuriakodis@phys.uoa.gr (G.-E. Kyriakodis).

http://dx.doi.org/10.1016/j.uclim.2017.02.002
2212-0955/

population and affect health conditions, while it raises the global ecological footprint of cities (Baccini et al., 2008; Pantavou et al., 2011; Sakka et al., 2012; Santamouris, 2015b; Santamouris and Kolokotsa, 2015; Santamouris et al., 2007; Stathopoulou et al., 2008). Recent studies have shown that the urban heat island increases the peak electricity demand during the summer period between 0.45% and 4.6% per degree of temperature increase (Santamouris et al., 2015b), while the annual energy consumption for cooling may increase up to 100% (Hassid et al., 2000; Santamouris et al., 2001). Compilation of the existing data on the energy penalty induced by the urban heat island has shown that it is close to 0.8 kW h per unit of city surface and degree of temperature increase or almost 68 kW h per person and degree (Santamouris, 2014b).

Forecasts of future cooling energy consumption of residential and commercial buildings reveal that by 2050 it may increase up to 750% and 275%, respectively, because of the local and global climate change, the tremendous increase of the population and the expected increase penetration of the cooling systems around the world (Santamouris, 2016a). To counterbalance the temperature increase in the urban environment and reduce as much as possible its impact on energy and environment, advanced and efficient mitigation technologies have been developed and applied widely (Akbari et al., 2016). Proposed mitigation technologies involve the use of reflective materials to solar radiation, additional urban greenery integrated into buildings and the city structure, dissipation of the excess urban heat into low temperature heat sinks like the ground and the water, solar shading, reduction of the anthropogenic heat and use of evaporation technologies (Akbari and Kolokotsa, 2016).

Highly reflective materials to solar radiation when used in the urban environment present a significantly lower surface temperature and contribute to reducing the sensible heat released in the atmosphere and mitigating the urban heat island (Doulos et al., 2004). Reflective or cool materials may be used on the roofs of urban buildings, cool roofs, and as pavements in the open urban spaces,cool pavements. Several types and technologies of cool materials for buildings and pavements have been developed involving reflective materials in the visible or infrared part of solar radiation (Synnefa et al., 2007, 2006), thermochromic coatings (Karlessi et al., 2009), reflective asphaltic products (Synnefa et al., 2011) reflective membranes and retroreflective materials (Pisello et al., 2016; Rossi et al., 2015; Santamouris et al., 2011), etc. Analysis of tens of studies and large scale applications have shown that the use of cool materials in the urban environment may decrease the average and peak ambient temperature up to 1.0 K and 2.5 K respectively (Santamouris, 2014a).

The development of reflective and/or pervious pavement may contribute significantly reducing the urban temperature and mitigating the urban heat island. Several technologies of reflective pavements have been developed and are commercially available while important research is carried out on the topic (Santamouris, 2013). Hundreds of large scale applications of reflective pavements are available around the world and their experimental evaluation shows that their mitigation potential is quite high (Castaldo et al., 2015; Fintikakis et al., 2011; Gaitani et al., 2011; Huynh and Eckert, 2012; OMalley et al., 2015; Santamouris et al., 2012; Tumini, 2014; Wang et al., 2016b). A recent analysis of 15 large scale mitigation projects involving the use of various types of reflective pavements has shown that the average and the peak temperature drop achieved was 1.3 K and 2.5 K, respectively (Santamouris et al., 2016), while the average and peak temperature drops per 10% increase of the albedo was close to 0.27 K and 0.94 K.

The existence and the characteristics of the urban heat island phenomenon is very well documented in the city of Athens, Greece (Livada et al., 2002; Mihalakakou et al., 2004). The phenomenon is more intense in the Western part of the city characterized by high urban density, increased anthropogenic heat, and lack of green spaces, and its magnitude may exceed 6–7 K (Giannopoulou et al., 2014; Mihalakakou et al., 2002). To counterbalance the significant impact of the high ambient temperatures in the area, a large scale rehabilitation program involving the use of various mitigation technologies has been designed and implemented (Santamouris et al., 2015a).

The present paper presents the design and the experimental evaluation of a large scale implementation of cool asphaltic and concrete pavements on a major traffic axis of Western Athens, covering a total zone of 37,000 m^2. The project is, to our knowledge, one of the largest urban mitigation projects in the world.

2. Description of the site

The rehabilitative area is the main traffic axis (Thivon Avenue) of the Municipality of Egaleo, situated in the western suburbs of Athens with the long axis in a NE′N-SW′S direction (6 7◦ from real North counter-clockwise) as Fig. 1 depicts. The geometrical characteristic of the traffic axis was L/W = 8. It consists of four traffic lanes separated with a refuge island with planted trees along its axis. Furthermore, both sides of the road are covered with pavements and there are three-to four-story buildings adjacent to them, which characterize the area as a mixed residential and industrial zone. The axis supports intensive traffic while the anthropogenic heat released is quite high. The road was initially covered with conventional black asphalt, while grey concrete tiles were used as pavements. The climate of the area corresponds to very hot and dry summers and it is influenced by the presence of mount Egaleo which acts as a natural obstacle against the northern winds, which dominate during the summer period in the Athens area. Detailed climatic monitoring of the area, has shown that the specific urban zone presents the high ambient temperature in the city of Athens (Giannopoulou et al., 2011). The project was carried out by the Prefecture of Athens in collaboration with the local Municipality and was built between 2014 and 2015. The renovation covers a total area of 37,000 m^2 and is the greatest recorded in Greece. It involves the implementation of approximately 18,000 m^2 of cool coloured thin layer asphalt and of approximately 19,300 m^2 of reflective concrete pavements.

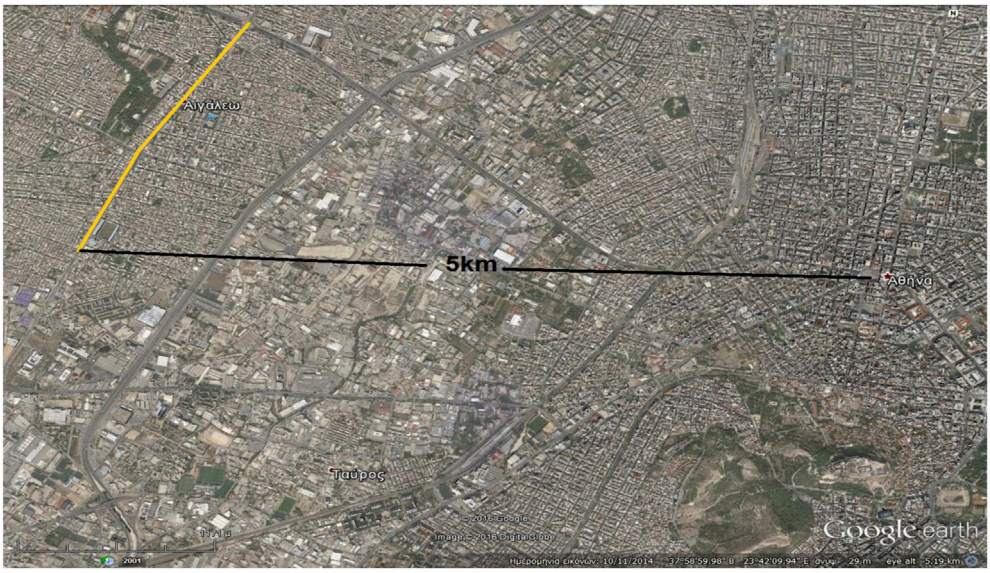

Fig. 1. Orientation of rehabilitative area, Egaleo, Athens.

3. Characteristics of the installed reflective pavements

Pavement materials were selected in order to:

(a) Improve as much as possible the thermal conditions in the area, mitigate the urban heat island and enhance thermal comfort conditions.
(b) Ensuring driving safety by avoiding undesirable contrast levels and glare.
(c) Ensuring the environmental remediation by reducing motor vehicle air pollutants (NO_2).

To satisfy the above objectives, the existing black conventional asphalt presenting a solar reflectance SR close to 0.04 was replaced by a light yellow thin layer asphalt characterized by SR = 0.35 and an emissivity close to 0.9 (Fig. 2). To avoid problems of contrast and glare, the material was designed to present much higher reflectivity in the near infrared than in the visible part of the solar radiation (Table 1). The yellow thin layer asphalt was developed by mixing an elastomeric asphalt binder with infrared reflective pigments and aggregates and the final application was achieved with slurry surfacing technique.

In parallel, the grey concrete pavements were replaced by white concrete pavements (SR = 0.66) mixed with pigments of TiO_2. The spectral reflectance of the pavements is given in Fig. 3, while a picture of the pavement tiles in the visible and infrared is given in Fig. 4. The infrared emittance of the pavements was measured as close to 0.9, according to the ASTM Standard E408-71: Standard Test Method for Total Normal Emittance of Surfaces. When exposed to sunlight and in the presence of a low concentration of water molecules, TiO_2 contained within the pavements generates hydroxyl radicals (OH), a powerful oxidizing agent. These radicals promote the oxidation of a variety of organic and inorganic pollutants (Wang et al., 2016a). Notably, the photocatalytic property of these pavements resulted to a 15% in oxidation of NO_X to NO_3 (Fig. 5).

The ageing of the materials and in particular the potential optical degradation and decrease of the reflectivity was assessed through continuous monitoring of their optical performance. The spectral reflectances of the materials were measured in the Materials Lab of the University of Athens, using a UV/vis/NIR spectrophotometer (Varian Carry 5000) fitted with a 150 mm diameter integrating sphere that collects both specular and diffuse radiation, according to the ASTM Standard E903-96: Standard Test Method for Solar Absorptance, Reflectance and Transmittance of Materials Using Integrating Spheres. It was found that after six months of continuous use, the reflectivity of the cool asphalt was reduced from 0.33 to 0.17 (Fig. 6). Decrease of the solar reflectance is attributed to the deposition of rubber from the tyres of cars on the surface of cool asphaltic materials just after their installation (Synnefa et al., 2011) and also to the decrease of the reflectivity of the cool pavements because of the deposition of several atmospheric pollutants on their surface (Mastrapostoli et al., 2016). It is observed that the cool asphaltic material recovers the initial reflectivity almost fully, (SR = 0.33), when scrubbing it with wet solvent (H_2O). In order to further investigate the specific optical degradation of the asphaltic material, Fourier Transform Infrared spectroscopy techniques were used to test the cleaner and the pollutant sample. FTIR measurements identified the existence of additional three band vibrations at: 3422.3, 1028.96, 470.21 cm^{-1} which label N–H, C–N and Pb–O bonds respectively. It is concluded that the contaminated samples were

Fig. 2. A picture of the installed yellow thin layer asphalt.

polluted by the particle compounds of motor vehicle emissions and the deposition of the tyres of vehicles. Contrary to the asphaltic material, the variation of the solar reflectivity of the concrete pavements was almost insignificant.

4. Monitoring campaign and experimental assessment

The experimental assessment, except for the laboratory measurements presented above, included an extensive monitoring strategy of in situ measurements in the area. Thence, a detailed monitoring campaign was scheduled in order to evaluate the impact of the implemented cool pavements in the microclimate of the area and to document the thermal performance of the selected materials compared to the conventional ones. The necessary values for the boundary conditions of the thermal model were also recorded.

The monitoring campaign was performed during the entirety of the summer period of May–September 2015 and at least three records per month were carried out based on the same experimental protocol. The outdoor climatic conditions of the experimental period were characterized by very hot days (approximating a heat wave) and typical clear sky conditions. We emphasized the time interval between 12:00 and 17:00 LST, due to these being the hours of maximum solar radiation and, consequently, the hours of maximum solar gains. Measurements of the ambient temperature and relative humidity were recorded with a data logger at a height of 1.5 m, placed in a thermometer shelter near the traffic axis. The accuracy of the thermometer was ±0.1 K. In parallel, the instantaneous values of surface temperatures were measured at time steps of 30 min (Fig. 7). The sample points of measurements were always the same, selected for not being shaded and providing assured access to different types of asphalt. It is worth stating that every two weeks, the cool coloured asphalt was cleaned by means of wet solvent (H_2O) scrubs at least one day before the initial measurement in order to eliminate evaporation effects. The reference points were the following:

Table 1
Solar reflectance values (SR, 300–2500nm) and solar reflectance values in the UV (300–400nm), vis (400–700nm) and IR (700–2500nm) part of the spectrum of cool light yellow and conventional black asphalt.

Sample	SR	SR_{UV}	SR_{VIS}	SR_{NIR}
Light yellow asphalt	0.35	0.11	0.24	0.42
Conventional black asphalt	0.04	0.04	0.03	0.04

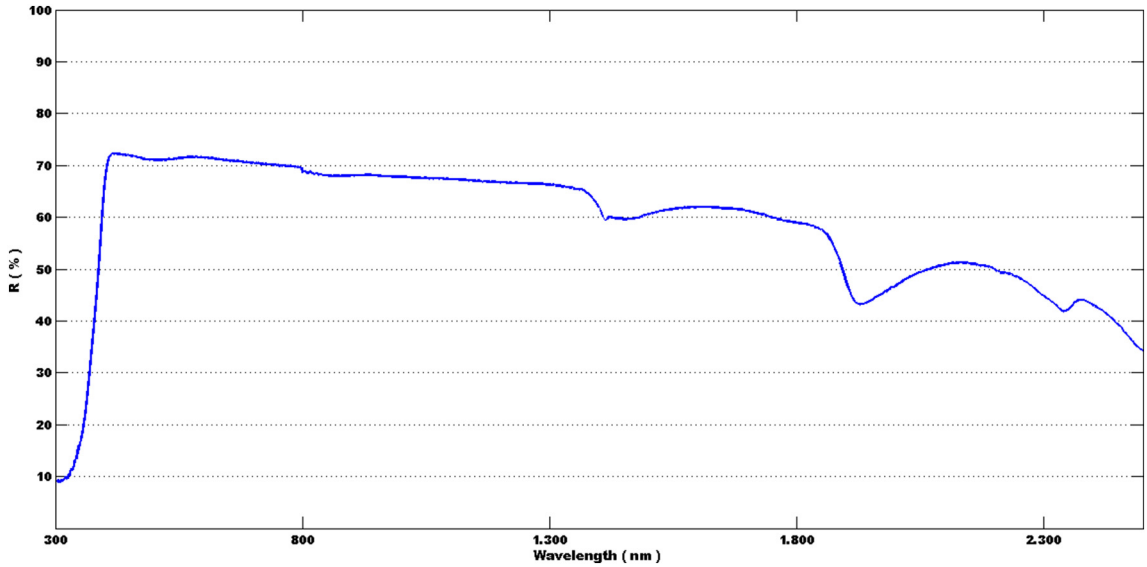

Fig. 3. The solar reflectance of the implemented pavements.

1. S_1 conventional black asphalt
2. S_2 conventional faint asphalt
3. S_3 light yellow cool asphalt
4. S_4 light yellow cool contaminated asphalt
5. S_{pl} cool photocatalytic pavement (coloured white)
6. S_{grey} conventional pavement (coloured grey).

The instruments used to depict surface temperature differences among sample points were an infrared camera (AGEMA Thermovision 570, 7.5–13 μm wavelength) and a visual IR Thermometer (Fluke VT02). The ambient climatic conditions were also recorded, while climatic data around the experimental site, including ambient temperature, relative humidity, wind speed and direction, global and direct solar radiation on a horizontal surface were collected from three meteorological stations of the NOA (National Observatory of Athens).

5. Monitoring results

On site comparative measurements revealed that the average surface temperature of the reflective asphalt over the cooling period is by up to 7.5 °C lower than the corresponding surface temperature of the conventional asphalt. In some cases of extremely hot conditions, the maximum temperature difference between the reflective and conventional asphalt could reach 11.5 °C. Almost similar results are reported in Synnefa et al. (2011), Carnielo and Zinzi (2013), Kawakami and Kubo (2008), Kondo et al. (2008), Nishioka et al. (2006). Fig. 8 reports the measurements taken on the 18th of July, considered as the most representative day of measurements for the entire summer.

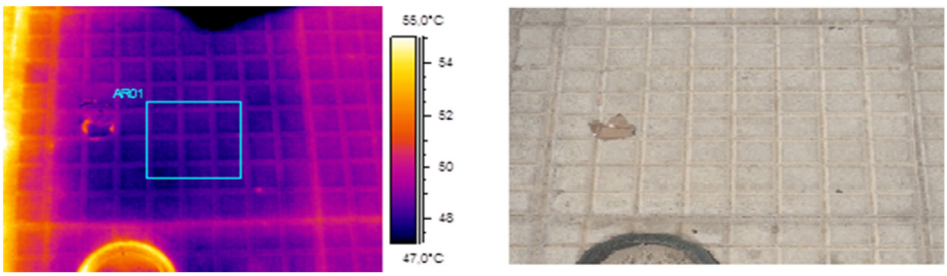

Fig. 4. Infrared and visible images of cool photocatalytic pavements (18/07/2015, 14:30LST) onsite.

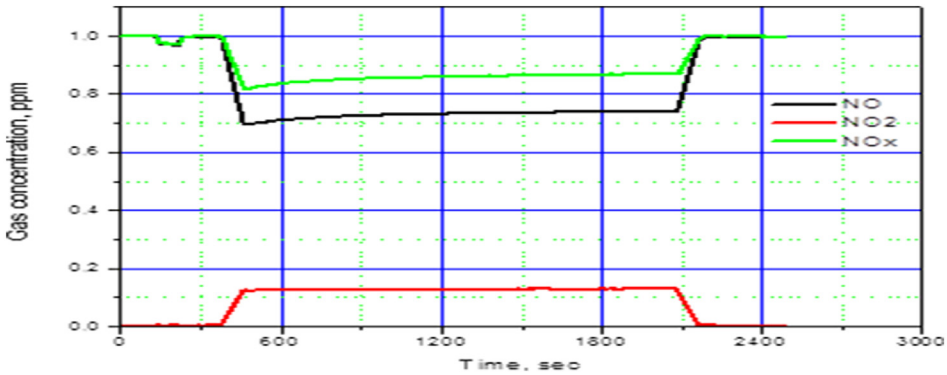

Fig. 5. The photocatalytic property of the implemented pavements.

Surface temperatures are found to present the same diurnal trend. Specifically, the maximum surface temperature of the black conventional asphalt was 68.5 °C, at 15:30 while, at the same time, the reflective light yellow asphalt was almost 8.9 °C lower, thus reaching 59.6 °C. During the measurement period, the differences between the reflective and conventional asphalt, varied between 7.5 and 8.9 °C and the average surface temperature difference was 8.3 °C. In parallel, the surface temperature of the polluted reflective and of the conventional faint asphalts presented a similar temporal trend. Maximum surface temperatures were measured at around 63.1 °C and 64.8 °C respectively. The average surface temperature reduction was close to 1.7 °C. Notably, the corresponding decrease depends on the sample point. In general, the relative decrease of the cooling period is approximately 3.0 °C. Fluctuations in measured values correspond to wind gusts. The daily variation of the concrete pavements followed the same trend as the asphaltic materials. The average surface temperature decrease of the reflective pavements was measured close to 6.1 °C, compared to the initially installed concrete pavement (Fig. 9).

In parallel, the average ambient temperature during the measurement time interval (10:00–18:00) in the area extracted by the sensor near the traffic axis and at 1.5 m height was 32.8 °C while the maximum value was recorded at 16:30 reaching 34.5 °C. Relative humidity measurements ranged between 22.3% (minimum 15:30) and 40% (maximum 11:00) presenting an average of 27.1% for the same time interval (Fig. 10). The corresponding measurements of the nearest meteorological station (elevation:50 m) also recorded the maximum at 16:30 presenting a value of 33.5 °C, while the average ambient temperature for the referenced time interval was 32.5 °C. As concerns solar radiation, the maximum value was recorded at 15:00 reaching the value of 844 W/m^2.

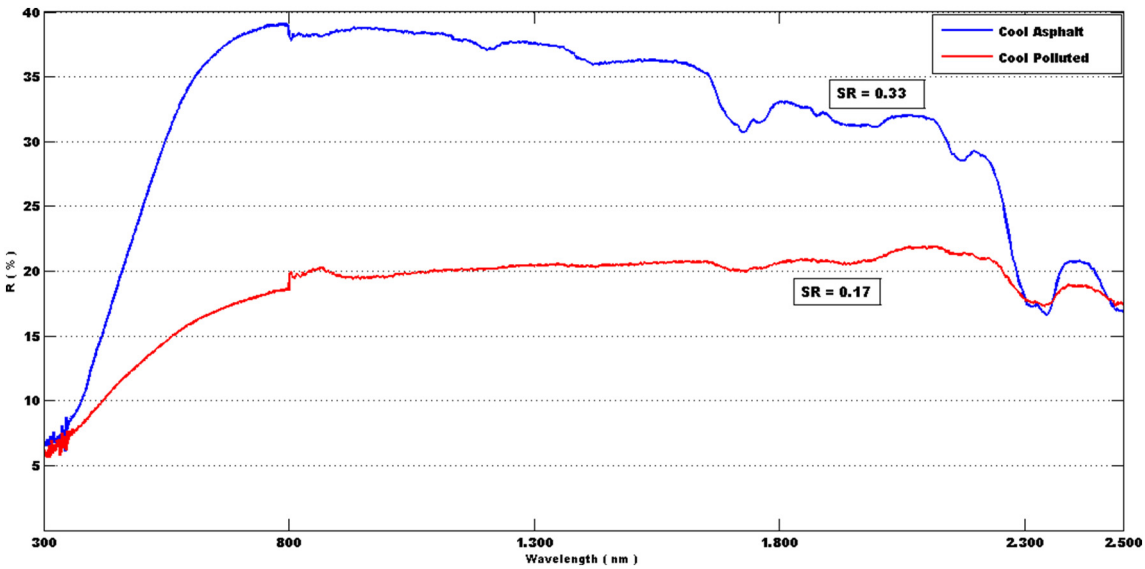

Fig. 6. Solar reflectance of clean (blue) and polluted (red) cool asphalt.

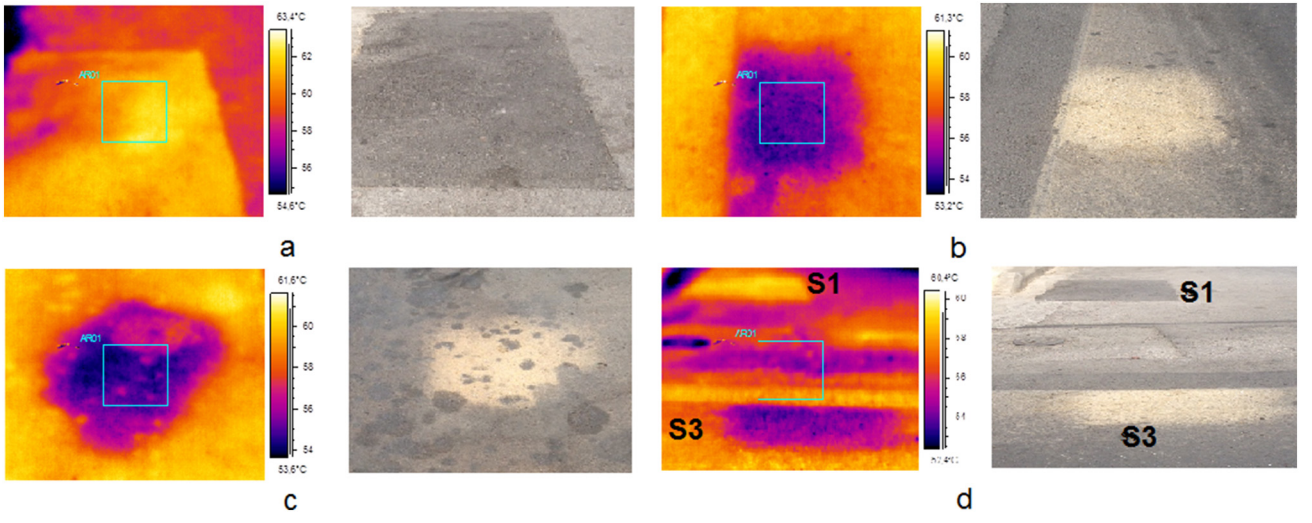

Fig. 7. Infrared and visible images of the conventional black (a), upstream cool (b), downstream cool (c) and comparison between them (18/07/2015, 14:00LST) onsite.

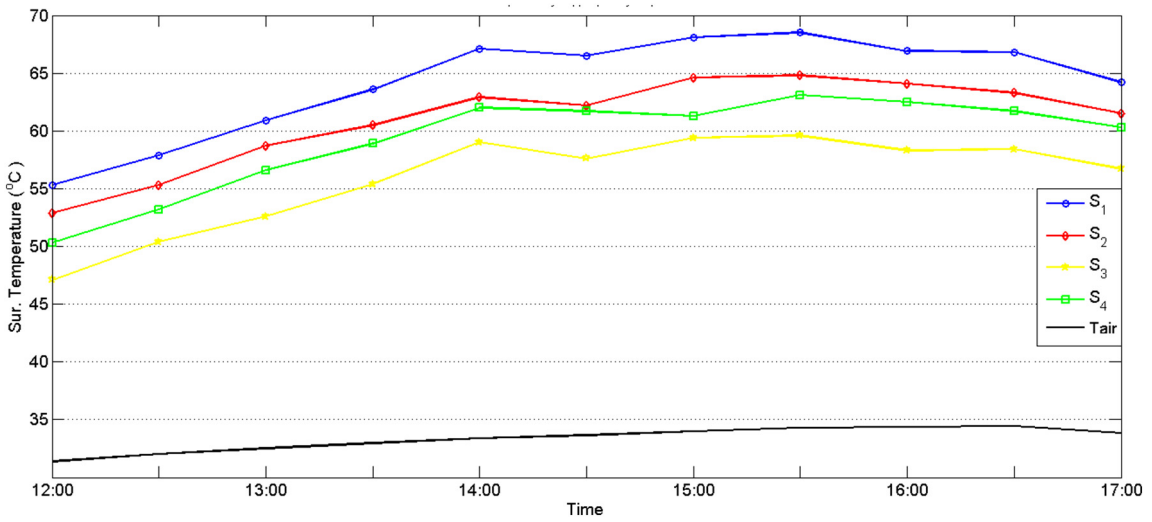

Fig. 8. Comparison of the measured surface temperatures of four different asphalt samples at the upstream in Thivon Avenue on 18th of July. Black curve depicts ambient temperature base.

6. Assessing the mitigation performance and the thermal improvements in the rehabilitated urban zone

A direct comparison of the experimental measurements performed before and after the climatic rehabilitation of a place is not possible given that measurements are taken under completely different climatic and boundary conditions. To overcome the problem, a specific methodology was proposed and applied in Santamouris et al. (2012). According to the proposed methodology, the collected experimental data are used to validate a numerical simulation model developed to predict the thermal performance in the considered area. The model is then used to simulate the thermal conditions in the area before and after the rehabilitation using exactly the same climatic and boundary conditions. A comparison of the two sets of calculated data permits to assess the achieved thermal improvements in the considered area.

A model of the urban zone with all specific details has been developed using the EnviMet Software (Bruse, 2004). ENVI-met is a three-dimensional microclimate model designed to simulate the surface-plant-air interactions with the urban environment. It is based on Reynolds Averaged Navier-Stokes (RANS) equations, with a non-hydrostatic, micro-scale, obstacle-resolving model and advanced parameterizations for simulation of surface-plant-air interactions in urban environments. ENVI-met provides both spatial resolution (0.5–10 m) and temporal variation (finest 10 s resolution) for an urban boundary layer climate. Additionally, ENVI-met has features not commonly available in other CFD dispersion codes (e.g. a detailed microclimate module and a vegetation module). The required input includes meteorological data and domain characteristics.

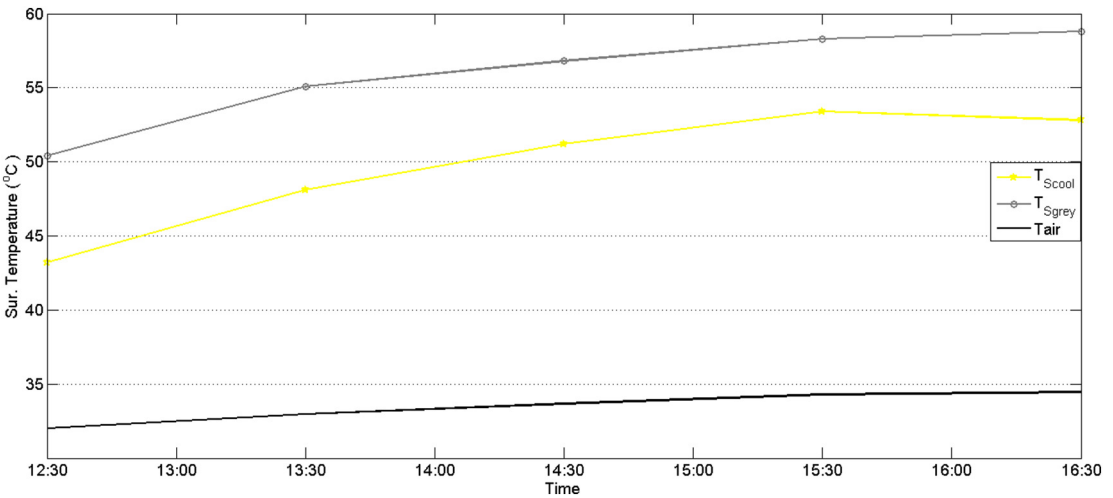

Fig. 9. Comparison of the measured surface temperatures of different pavement samples on 18th of July. Black curve depicts base ambient temperature.

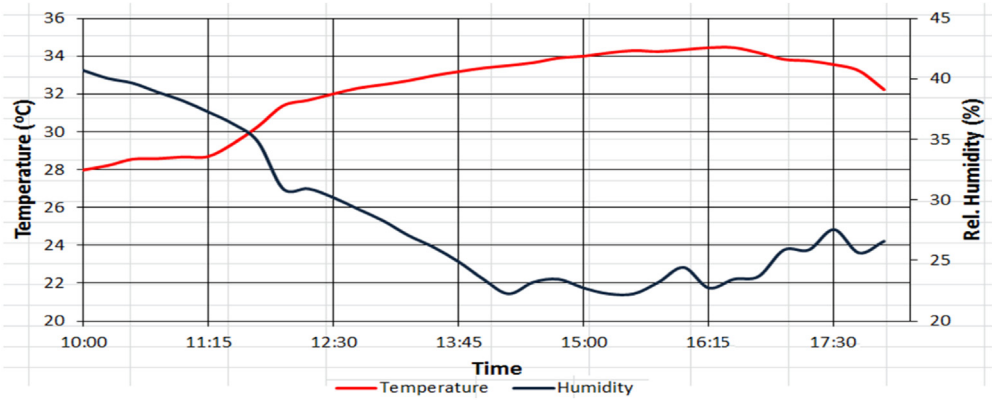

Fig. 10. Ambient climatic conditions for the 18th of July.

Fig. 11. Geometry and calculation domain (a), satellite image (b) of the simulated area.

The physical dimensions of the site correspond to a 1800(x) × 224(y) × 150(z) m and the calculation domain consists of 576 × 80 × 30 cells at each axis respectively (Fig. 11). Through the limited resolution that the non commercial basic version provides, the main domain was split into three sub-areas of equidistance length each. The scenario of changing the horizontal grid size (dx,dy) was deemed unacceptable. Otherwise, it would have been near impossible to consider the planted refuge island which has great impact on surface temperatures. Therefore, the dimensions of each sub-area consist of 192 × 80 × 30 cells. Note that the model area is rotated 293.4° out of grid north. In order to avoid numerical problems because of the interference of the model borders with internal model dynamics, seven additional nesting grids were included. Concerning turbulence, the 1.5 order E-epsilon turbulence closure model is used. At the outflow and lateral boundaries, a zero gradient condition was used, while at

Table 2
Input data of the configuration file.

Building properties	Values
Inside temperature [K]	301
Heat transmission walls [W/m^2 K]	1.1
Heat transmission roofs [W/m^2 K]	1.1
Albedo walls	0.2
Albedo roofs	0.2

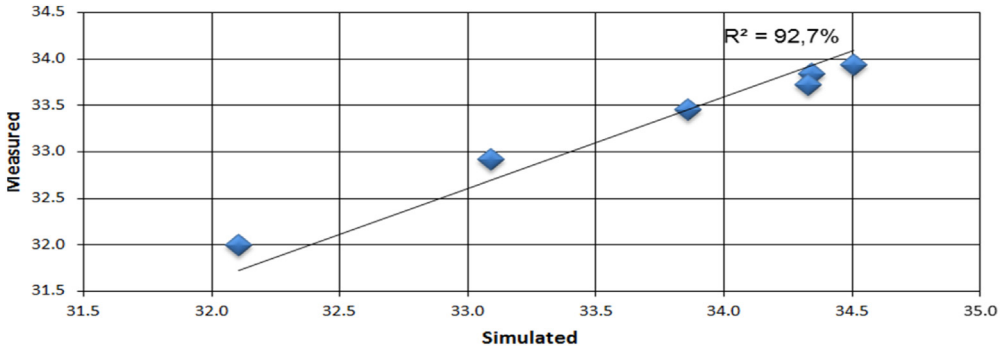

Fig. 12. Hourly simulated vs. measured air temperature for the 14th of June.

the top boundary, all vertical motions were assumed to be zero. The calculation of the variations of lateral boundary conditions (LBC) of temperature and humidity was chosen to be the "open" method. With this method, the values of the next grid point close to the border are copied to the border at each time step (Kawakami and Kubo, 2008). The variation of lateral boundary condition of kinetic energy of the air inflow was instead calculated with the "forced" method by which the values of the one dimensional model are copied to the border. In addition, for the accomplishment of the configuration file, imports concerning inside temperature and thermophysical properties of the buildings were introduced, as shown in Table 2, in accordance with the characteristics of the majority of the buildings in the site.

Simulations were performed for different measured boundary conditions in order to better corroborate the real conditions. Thus, the 14th of June was preferred because it appeared to have an increased ambient temperature and better presented the summer climatic conditions in the area. The wind at a height of 10 m was measured to be a leading north wind of 1.9 m/s, while the roughness length (z_0) was estimated to be 0.6 according to Bruse and Fleer (1998). The solar radiation adjustment factor was set to 0.9 to simulate the intense radiation level of the specific clear summer day in Athens. For the initial air temperature, the value of 305.5 K was used. Three scenarios are simulated. The first scenario corresponded to the initial conditions before the climatic rehabilitation, the second and third scenarios described the specific conditions after the rehabilitation taking into account or neglecting the optical degradation of the materials respectively, (cool and aged cool scenarios). The calculated distribution of the surface and ambient temperature, as obtained from the second scenario, were compared with the corresponding measurements in order to achieve the best possible calibration of the model. An acceptable agreement between the experimental and theoretical results was obtained and the maximum difference of the ambient and surface temperatures did not exceed 0.4 K and 0.8 K, respectively. Fig. 12 presents the correlation between the simulated and measured values of the ambient temperature. The R^2 index was calculated equal to 92.7%.

Since the model was calibrated and validated, simulations were performed for the three scenarios as mentioned above and for each sub-area resulting in nine final simulations in total. Simulations have shown that the implemented reflective asphaltic material can effectively reduce the surface temperatures on a summer day, even if its reflectivity is reduced because of the ageing processes. In particular, the non aged asphaltic material, (albedo of 0.35), presented up to 9.0 K lower temperature than the conventional asphalt, (Table 3), while the lower albedo asphalt, (albedo of 0.17), had up to 6 K lower surface temperature than the conventional material (Table 4). In parallel, the surface temperature of the concrete pavements, (albedo 0.66), found to present up to 6 K lower temperature than the conventional grey pavement materials. Fig. 13, presents the predicted spatial distribution of the surface temperatures in each sub-area (14:00, 14/06/2015) for the previous (conventional), current (cool aged) and ideal (cool cleaned) condition vertically arranged. The last horizontal set depicts the spatial distribution of absolute differences in surface temperatures between cool cleaned and conventional materials.

As concerns the distribution of the ambient temperature in the considered area, simulations have shown that the application of the reflective pavements can significantly reduce the local air temperature. When the non aged asphaltic materials, (SR = 0.35) and the cool pavements are considered, cool scenario, the average maximum ambient temperature drop was close to 1.5 °C. For the conventional scenario, the ambient temperature at 1.5 m height is found to range between 32.9 °C

Table 3
Measured and predicted surface temperature differences of conventional and cool asphalt for the first subarea.

Time	Asphalt temperature (°C)	
	ΔT_{Cool}^{Conv} measured	ΔT_{Cool}^{Conv} predicted
12:00	7.3	7.4–7.9
14:00	8.2	8.2–9.0

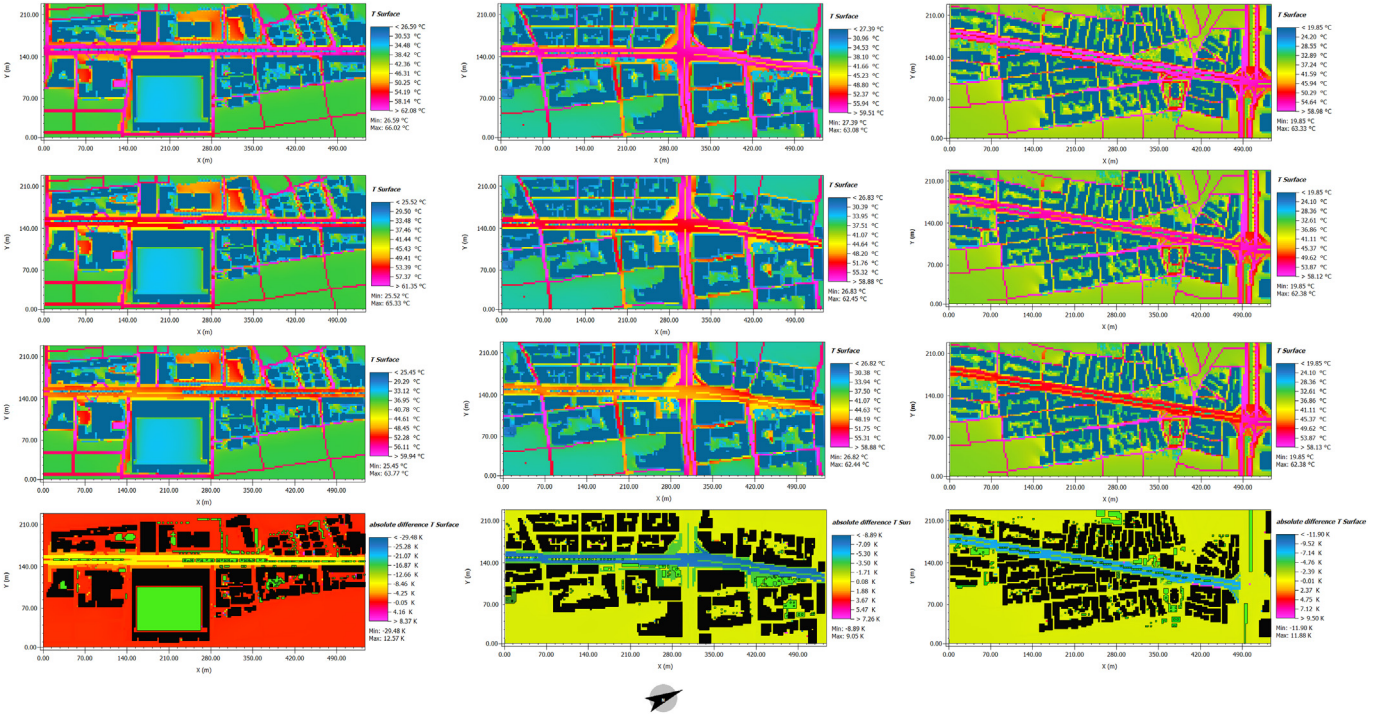

Fig. 13. Predicted spatial distribution of surface temperatures in each sub-area (14:00, 14/06/2015) for the previous (conventional), current (cool polluted) and ideal (cool cleaned) condition, vertically arranged. The last horizontal set depicts the spatial distribution of absolute difference in surface temperatures between cool cleaned and conventional materials.

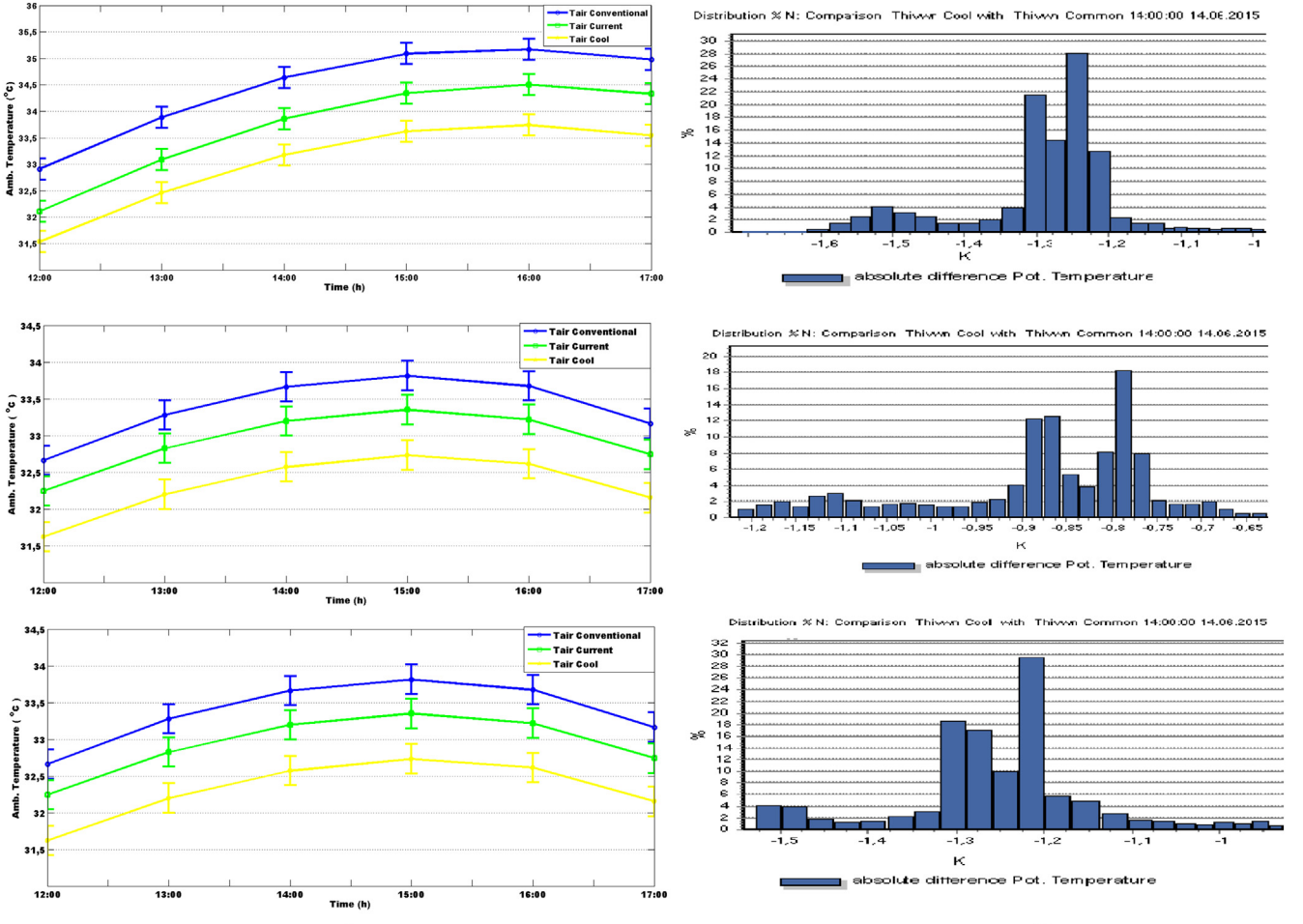

Fig. 14. A depicts predicted potential temperatures in each sub-area (14:00, 14/06/2015) for the previous (blue), current (green) and ideal (yellow) condition vertically arranged. B presents the (%) distribution of absolute difference in potential temperature of cool and conventional materials.

Table 4
Measured and predicted surface temperature of conventional, cool, and cool polluted asphalts for the first subarea.

Time	Temperature (°C)								
	Conventional			Cool			Current		
	Meas	Pred	ΔT	Meas	Pred	ΔT	Meas	Pred	ΔT
12:00	49.0	49.21	0.21	41.7	42.30	0.60	45.9	46.18	0.28
14:00	60.9	61.75	0.85	52.7	53.30	0.60	57.8	58.80	1.00

(12:00 LST) and 35.2 °C (maximum, 16:00 LST), while the respective ambient temperature for the cool scenario varied between 31.9 °C and 33.9 °C (Fig. 14). For the scenario in which the cool aged asphaltic material (SR = 0.17) is taken into account, cool aged scenario, the average maximum ambient temperature drop was 0.8 °C. The ambient temperature is found to range between 32.1 °C (12:00 LST) and 34.5 °C (maximum, 16:00 LST) presenting a reduction of 0.8 °C and 0.7 °C respectively compared to the conventional scenario (See Table 4).

7. Conclusions

Urban heat island effect and local climate change increase the ambient temperature of the cities, resulting on a significant impact on the energy consumption of buildings and adverse effects on vulnerable low income population, indoor and outdoor thermal comfort and health conditions. To counterbalance the effect, a large scale implementation of cool asphaltic and concrete pavements in a major traffic axis of Western Athens, covering a total zone of 37,000 m^2 has been designed and applied, resulting in one of the largest urban mitigation projects in the world. An efficient monitoring strategy was conducted in the area during the entirety of the summer period (May–September). It was found that cool materials demonstrated lower surface temperatures compared to the conventional ones and the amount of reduction reached 7.5 °C and 6.1 °C respectively in the summer period. The collected experimental data were used to validate a numerical simulation model developed to predict the thermal performance in the considered area. Three scenarios were simulated in order to depict the conditions before, conventional scenario, the current conditions, cool aged scenario, and the ideal, cool non aged scenario. It is concluded that the installed cool paving materials present a very high potential to decrease the sensible heat released to the atmosphere, while the maximum ambient temperature reduction approached 1.5 °C. Uncontestably, the whole bioclimatic rehabilitation project established that cool materials, as an application in open spaces, can reduce effectively the intensity of urban heat island effect and contribute to protect in a more effective way the local vulnerable population.

References

Akbari, H., Cartalis, C., Kolokotsa, D., Muscio, A., Pisello, A.L., Rossi, F., Santamouris, M., Synnefa, A., Wong, N.H., Zinzi, M., 2016. Local climate change and urban heat island mitigation techniques-the state of the art. J. Civ. Eng. Manag. 22 (1), 1–16.

Akbari, H., Kolokotsa, D., 2016. Three decades of urban heat islands and mitigation technologies research. Energ. Buildings 133, 834–842.

Baccini, M., Biggeri, A., Accetta, G., Kosatsky, T., Katsouyanni, K., Analitis, A., Anderson, H.R., Bisanti, L., D'Ippoliti, D., Danova, J., et al. 2008. Heat effects on mortality in 15 European cities. Epidemiology 19 (5), 711–719.

Bruse, M., 2004. Updated Overview Over ENVI-met 3.0. Acessado em 8 2008 http://www.envi-met.com.

Bruse, M., Fleer, H., 1998. Simulating surface-plant-air interactions inside urban environments with a three dimensional numerical model. Environ. Model Softw. 13 (3), 373–384.

Carnielo, E., Zinzi, M., 2013. Optical and thermal characterisation of cool asphalts to mitigate urban temperatures and building cooling demand. Build. Environ. 60, 56–65.

Castaldo, V., Coccia, V., Cotana, F., Pignatta, G., Pisello, A., Rossi, F., 2015. Thermal-energy analysis of natural "cool" stone aggregates as passive cooling and global warming mitigation technique. Urban Clim. 14, 301–314.

Doulos, L., Santamouris, M., Livada, I., 2004. Passive cooling of outdoor urban spaces. The role of materials. Sol. Energy 77 (2), 231–249.

Fintikakis, N., Gaitani, N., Santamouris, M., Assimakopoulos, M., Assimakopoulos, D.N., Fintikaki, M., Albanis, G., Papadimitriou, K., Chryssochoides, E., Katopodi, K., et al. 2011. Bioclimatic design of open public spaces in the historic centre of Tirana, Albania. Sustain. Cities Soc. 1 (1), 54–62.

Gaitani, N., Spanou, A., Saliari, M., Synnefa, A., Vassilakopoulou, K., Papadopoulou, K., Pavlou, K., Santamouris, M., Papaioannou, M., Lagoudaki, A., 2011. Improving the microclimate in urban areas: a case study in the centre of Athens. Build. Serv. Eng. Res. Technol. 32 (1), 53–71.

Giannopoulou, K., Livada, I., Santamouris, M., Saliari, M., Assimakopoulos, M., Caouris, Y., 2011. On the characteristics of the summer urban heat island in Athens, Greece. Sustain. Cities Soc. 1 (1), 16–28.

Giannopoulou, K., Livada, I., Santamouris, M., Saliari, M., Assimakopoulos, M., Caouris, Y., 2014. The influence of air temperature and humidity on human thermal comfort over the greater Athens area. Sustain. Cities Soc. 10, 184–194.

Hassid, S., Santamouris, M., Papanikolaou, N., Linardi, A., Klitsikas, N., Georgakis, C., Assimakopoulos, D.N., 2000. The effect of the Athens heat island on air conditioning load. Energ. Buildings 32 (2), 131–141.

Huynh, C., Eckert, R., 2012. Reducing heat and improving thermal comfort through urban design-a case study in Ho Chi Minh City. Int. J. Environ. Sci. Dev. 3 (5), 480.

Karlessi, T., Santamouris, M., Apostolakis, K., Synnefa, A., Livada, I., 2009. Development and testing of thermochromic coatings for buildings and urban structures. Sol. Energy 83 (4), 538–551.

Kawakami, A., Kubo, K., 2008. Development of a cool pavement for mitigating the urban heat island effect in Japan. ISAP Symp. pp. 423–434.

Kondo, Y., Ogasawara, T., Kanamori, H., 2008. Field measurements and heat budget analysis on sensible heat flux from pavement reduction of sensible heat emission by cool pavement as countermeasure of heat island (part 1). J. Environ. Eng. (Trans. AIJ) 73 (628), 791–797.

Livada, I., Santamouris, M., Niachou, K., Papanikolaou, N., Mihalakakou, G., 2002. Determination of places in the great Athens area where the heat island effect is observed. Theor. Appl. Climatol. 71 (3-4), 219–230.

Mastrapostoli, E., Santamouris, M., Kolokotsa, D., Vassilis, P., Venieri, D., Gompakis, K., 2016. On the ageing of cool roofs: measure of the optical degradation, chemical and biological analysis and assessment of the energy impact. Energ. Buildings 114, 191–199.
Mihalakakou, G., Flocas, H.A., Santamouris, M., Helmis, C.G., 2002. Application of neural networks to the simulation of the heat island over Athens, Greece, using synoptic types as a predictor. J. Appl. Meteorol. 41 (5), 519–527.
Mihalakakou, G., Santamouris, M., Papanikolaou, N., Cartalis, C., Tsangrassoulis, A., 2004. Simulation of the urban heat island phenomenon in Mediterranean climates. Pure Appl. Geophys. 161 (2), 429–451.
Nishioka, M., Nabeshima, M., Wakama, S., Ueda, J., 2006. Effects of surface temperature reduction and thermal environment on high albedo coating asphalt pavement. J. Heat Island Inst. Int. 1, 46–52.
OMalley, C., Piroozfar, P., Farr, E.R., Pomponi, F., 2015. Urban heat island (UHI) mitigating strategies: a case-based comparative analysis. Sustain. Cities Soc. 19, 222–235.
Pantavou, K., Theoharatos, G., Mavrakis, A., Santamouris, M., 2011. Evaluating thermal comfort conditions and health responses during an extremely hot summer in Athens. Build. Environ. 46 (2), 339–344.
Pisello, A.L., Castaldo, V., Pignatta, G., Cotana, F., Santamouris, M., 2016. Experimental in-lab and in-field analysis of waterproof membranes for cool roof application and urban heat island mitigation. Energ. Buildings 114, 180–190.
Rossi, F., Castellani, B., Presciutti, A., Morini, E., Filipponi, M., Nicolini, A., Santamouris, M., 2015. Retroreflective façades for urban heat island mitigation: experimental investigation and energy evaluations. Appl. Energy 145, 8–20.
Sakka, A., Santamouris, M., Livada, I., Nicol, F., Wilson, M., 2012. On the thermal performance of low income housing during heat waves. Energ. Buildings 49, 69–77.
Santamouris, M., 2001. Energy and Climate in the Urban Built Environment. James and James Science Publishers.
Santamouris, M., 2013. Using cool pavements as a mitigation strategy to fight urban heat island-a review of the actual developments. Renew. Sust. Energ. Rev. 26, 224–240.
Santamouris, M., 2014a. Cooling the cities-a review of reflective and green roof mitigation technologies to fight heat island and improve comfort in urban environments. Sol. Energy 103, 682–703.
Santamouris, M., 2014b. On the energy impact of urban heat island and global warming on buildings. Energ. Buildings 82, 100–113.
Santamouris, M., 2015a. Analyzing the heat island magnitude and characteristics in one hundred Asian and Australian cities and regions. Sci. Total Environ. 512, 582–598.
Santamouris, M., 2015b. Regulating the damaged thermostat of the cities-status, impacts and mitigation challenges. Energ. Buildings 91, 43–56.
Santamouris, M., 2016a. Cooling the buildings-past, present and future. Energ. Buildings 128, 617–638.
Santamouris, M., 2016b. Innovating to zero the building sector in Europe: minimising the energy consumption, eradication of the energy poverty and mitigating the local climate change. Sol. Energy 128, 61–94.
Santamouris, M., Cartalis, C., Synnefa, A., 2015a. Local urban warming, possible impacts and a resilience plan to climate change for the historical center of Athens, Greece. Sustain. Cities Soc. 19, 281–291.
Santamouris, M., Cartalis, C., Synnefa, A., Kolokotsa, D., 2015b. On the impact of urban heat island and global warming on the power demand and electricity consumption of buildings-a review. Energ. Buildings 98, 119–124.
Santamouris, M., Ding, L., Fiorito, F., Oldfield, P., Osmond, P., Paolini, R., Prasad, D., Synnefa, A., 2016. Passive and active cooling for the outdoor built environment - analysis and assessment of the cooling potential of mitigation technologies using performance data from 220 large scale projects. Sol. Energy (in press).
Santamouris, M., Gaitani, N., Spanou, A., Saliari, M., Giannopoulou, K., Vasilakopoulou, K., Kardomateas, T., 2012. Using cool paving materials to improve microclimate of urban areas-design realization and results of the flisvos project. Build. Environ. 53, 128–136.
Santamouris, M., Kolokotsa, D., 2015. On the impact of urban overheating and extreme climatic conditions on housing, energy, comfort and environmental quality of vulnerable population in Europe. Energ. Buildings 98, 125–133.
Santamouris, M., Kolokotsa, D., 2016. Urban Climate Mitigation Techniques. Routledge.
Santamouris, M., Papanikolaou, N., Livada, I., Koronakis, I., Georgakis, C., Argiriou, A., Assimakopoulos, D.N., 2001. On the impact of urban climate on the energy consumption of buildings. Sol. Energy 70 (3), 201–216.
Santamouris, M., Paraponiaris, K., Mihalakakou, G., 2007. Estimating the ecological footprint of the heat island effect over Athens, Greece. Clim. Chang. 80 (3-4), 265–276.
Santamouris, M., Synnefa, A., Karlessi, T., 2011. Using advanced cool materials in the urban built environment to mitigate heat islands and improve thermal comfort conditions. Sol. Energy 85 (12), 3085–3102.
Stathopoulou, E., Mihalakakou, G., Santamouris, M., Bagiorgas, H., 2008. On the impact of temperature on tropospheric ozone concentration levels in urban environments. J. Earth Syst. Sci. 117 (3), 227–236.
Synnefa, A., Karlessi, T., Gaitani, N., Santamouris, M., Assimakopoulos, D.N., Papakatsikas, C., 2011. Experimental testing of cool colored thin layer asphalt and estimation of its potential to improve the urban microclimate. Build. Environ. 46 (1), 38–44.
Synnefa, A., Santamouris, M., Apostolakis, K., 2007. On the development, optical properties and thermal performance of cool colored coatings for the urban environment. Sol. Energy 81 (4), 488–497.
Synnefa, A., Santamouris, M., Livada, I., 2006. A study of the thermal performance of reflective coatings for the urban environment. Sol. Energy 80 (8), 968–981.
Tumini, I., 2014. The urban microclimate in open space. Case Studies in Madrid Cuadernos de investigación urbanística. 96. pp. 1–73.
Wang, D., Leng, Z., Hüben, M., Oeser, M., Steinauer, B., 2016a. Photocatalytic pavements with epoxy-bonded TiO_2-containing spreading material. Constr. Build. Mater. 107, 44–51.
Wang, Y., Berardi, U., Akbari, H., 2016b. Comparing the effects of urban heat island mitigation strategies for Toronto, Canada. Energ. Buildings 114, 2–19.